Role of Adsorption in the Permeation of CH 4 and CO 2 through a Silicalite1 Membrane

ARTICLE *in* INDUSTRIAL & ENGINEERING CHEMISTRY RESEARCH · JANUARY 2006

Impact Factor: 2.59 · DOI: 10.1021/ie0507427

Role of Adsorption in the Permeation of CH_4 and CO_2 through a Silicalite-1 Membrane

Weidong Zhu,*,† Pavel Hrabanek,† Leszek Gora,‡ Freek Kapteijn,† and Jacob A. Moulijn†

Reactor & Catalysis Engineering, DelftChemTech, and Ceramic Membrane Centre, The Pore, Delft University of Technology, Julianalaan 136, 2628 BL Delft, The Netherlands

The role of adsorption in the single and binary permeation of CH_4 and CO_2 through a silicalite-1 membrane has been investigated. Adsorption on the zeolite is favorable for CO_2, resulting in selectivity for CO_2 in the permeation. The generalized Maxwell−Stefan (GMS) equations, in combination with the ideal adsorbed solution theory (IAST), were used to model their binary permeation. It is found that the use of accurate adsorption data is of utmost importance for extracting transport properties from the single-component permeation as well as for modeling multicomponent permeation. The GMS model qualitatively and quantitatively predicts the temperature-dependent properties of the mixture permeation, while it slightly deviates from the experimental observation on the pressure dependence of the mixture selectivity. This deviation is ascribed to intercrystalline or surface barriers for the larger molecule CH_4 in the membrane as well as to the overprediction of the CO_2 loading in the zeolite by the IAST.

1. Introduction

Separation and recovery of CO_2 from natural gas are of great interest. Natural gas is a complex mixture containing desirable gaseous hydrocarbons (mainly CH_4) and non-hydrocarbon components such as CO_2, H_2S, and H_2O. Removal of the acidic gases CO_2 and H_2S from the desired lower hydrocarbons is an important processing operation, since they can corrode pipelines as well as reduce the energy content of the gas.[1] Development of effective separation technologies for removal of CO_2 from natural gas is still a challenging research topic.

In the past decades, membrane technology has been considered as an attractive alternative to conventional separation processes such as filtration, purification, and cryogenic distillation, because of its low energy consumption and compact design. Polyimide membranes have been used for CO_2/CH_4 separation because of their good mechanical and gas separation properties.[2] However, because of CO_2-induced plasticization, the permeability or permeance increases, while the selectivity decreases. The plasticization-induced selectivity drop, therefore, presents one of the most severe technical challenges, when one considers commercializing a new membrane system for CO_2/CH_4 separation. Zeolite membranes have the potential to eliminate this disadvantage, because they are chemically stable for such a component. Some investigators indeed have studied the separation of CO_2 and CH_4 by zeolite membranes. Falconer and co-workers[3−8] used SAPO-34 membranes to separate CO_2 and CH_4 mixtures and found that the highest selectivity for CO_2 was 270 at 253 K.[8] However, the selectivity and CO_2 flux through these membranes were significantly reduced by the presence of water,[5] which is present in natural gas, because the SAPO-34 zeolite is hydrophilic in nature and has a strong affinity to water adsorption. To prevent the negative effect of water adsorption on the purification of natural gas, the zeolite membranes should be hydrophobic. Recently, Tomita et al.[9] found that a DD3R membrane was suitable for the purification of CO_2 from natural gas: high selectivity and flux for CO_2 and a negligible effect of water on the performance.

MFI-type membranes have been extensively studied so far. This is due to the accumulated knowledge of the synthesis, the suitable channel-opening size, and a high thermal stability. Several investigators have studied the single and/or binary permeation of CH_4 and CO_2 through MFI-type membranes.[10−22] In most of the reported work, the purpose was to use CH_4 and CO_2 as probes to characterize the quality of the synthesized MFI-type membranes. If large defects are present in the membranes, the ideal and mixture selectivity will be favorable for CH_4, which is attributed to pores with Knudsen (and viscous) flow. In general, the membranes with larger permeation through nonzeolite pores have higher CH_4/CO_2 selectivity. On the other hand, the selectivity will be favorable for CO_2 for the permeation through the defect-free membranes. This is ascribed to the favorable adsorption of CO_2 over CH_4 in the zeolite. Poshusta et al.[15] reported that the CO_2/CH_4 (50:50) mixture selectivity was 5.5 at room temperature and decreased with temperature because of a decrease in competitive adsorption.

Besides a major emphasis on the further development of the preparation methods, the search for new membrane types based on other zeolites, and the demonstration of the potential separation properties, an understanding of transport phenomena in microporous membranes is highly desired. To be able to quantitatively describe the membrane behavior in terms of permeation fluxes and selectivity with the purpose to design separation and reaction units, good engineering models are needed. But, up to now, only limited work has dealt with the modeling of CO_2 and CH_4 permeation through MFI-type membranes. Bakker et al.[12] proposed a surface-diffusion model in combination with activated gas diffusion to explain the temperature dependence of single-component fluxes (permeances); at low temperatures, the transport of the permeating species through a silicalite-1 membrane is dominated by the surface diffusion, while at high temperatures, the activated gas diffusion starts controlling the permeation process. This predicts the correct temperature dependence of the single-component permeation. Van den Broeke et al.[18] used the generalized Maxwell−Stefan (GMS) equations to model the component fluxes and the separation factor of CO_2 and CH_4 mixture

* To whom correspondence should be addressed. Tel.: 0031-15-2784316. Fax: 0031-15-2785006. E-mail: w.zhu@tnw.tudelft.nl.

† Reactor & Catalysis Engineering, DelftChemTech.

‡ Ceramic Membrane Centre, The Pore.

10.1021/ie0507427 CCC: $33.50
Published on Web 11/11/2005

permeation through a silicalite-1 membrane. In their modeling, two types of mixture isotherms, based on the ideal adsorbed solution theory (IAST) and the extended Langmuir model, were examined, and the "single-file" diffusion that is a special case of the GMS equations for micropore diffusion was adopted. The results showed that the GMS equations in combination with the IAST better described the binary permeation of CO_2 and CH_4 through the membrane. However, the authors did not show details regarding the role of adsorption in the modeling.

In general, diffusivities can be determined by measuring single-component fluxes, based on separately determined pure-component isotherms. In this manner, any uncertainty in the used isotherms will pass on the determined transport properties. Often single-component isotherms and derived diffusivities as input are used to model multicomponent permeation.[23] Therefore, the use of accurate adsorption data is of utmost importance for extracting transport properties from the membrane permeation as well as for modeling multicomponent permeation. In the current study, first, the isotherms of CH_4 and CO_2 will be presented and compared with available literature data. Then, single- and binary-permeation results are shown for CH_4 and CO_2 across a high-quality silicalite-1 membrane. On the basis of the measured equilibrium adsorption data of the pure components, the transport parameters are derived from the unary permeation. The model, based on the GMS equations in combination with the IAST, is presented in detail, and it is used to simulate the component fluxes and the separation factors of the binary mixtures as a function of temperature and total feed pressure. A comparison with experimental data is made to verify the model. Finally, the feasibility of zeolite membranes as applied to CO_2/CH_4 separation is anticipated.

2. Modeling

2.1. Adsorption. The Langmuir isotherm is often used to describe adsorption on microporous materials,

$$q = q^{sat}\frac{Kp}{1+Kp} \quad \text{or} \quad \theta = \frac{Kp}{1+Kp} \tag{1}$$

The value of the saturation capacity q^{sat} should remain constant for all temperatures. The adsorption equilibrium constant K is temperature dependent, taking the usual van't Hoff relation that can be written as

$$K = K_0 \exp\left(\frac{-\Delta H_{ads}}{R_g T}\right) \tag{2}$$

For practical utility, the experimental data should be correlated with an analytical expression that includes adjustable parameters as a function of temperature. Therefore, the nonlinear parameter estimation will be carried out and the parameters q^{sat}, K_0, and ΔH_{ads} will be simultaneously estimated from the isotherm data at all temperatures by eqs 1 and 2, called the combined fitting.

The Henry law constant K_H quantifies the extent of adsorption for a given adsorptive by a solid. The magnitude of K_H depends on the properties of both adsorptive and solid. For the Langmuir isotherm, K_H can be expressed by the following formula:

$$K_H = q^{sat}K = q^{sat}K_0 \exp\left(\frac{-\Delta H_{ads}}{R_g T}\right) \tag{3}$$

From the calculated values of K_H at multiple temperatures, the isosteric heat at zero coverage can be derived from its definition, and its value is equal to $-\Delta H_{ads}$.

The IAST developed by Myers and Prausnitz[24] can be used to predict the adsorption equilibrium of gas mixtures on the basis of pure gas-adsorption isotherms only. The equilibrium between the two-dimensional adsorbed phase, which is considered to be an ideal solution, and a perfect gas phase is described by an equation analogous to Raoult's law for vapor−liquid equilibria. Because the IAST is thermodynamically consistent, it is often applied to the prediction of mixture adsorption.

2.2. Permeation. The permeation across a silicalite-1 membrane, based on the Wicke−Kallenbach method, is considered. The membrane separates two well-mixed compartments, as defined in the literature.[23] A "defect-free" membrane is assumed, the mass-transfer resistances external to the membrane are ignored, and the transfer fluxes are determined solely by intramicroporous membrane transport. For a homogeneous membrane under isothermal conditions, the fluxes of permeating species through the membrane are given by the GMS equations. The detailed expressions can be found in the literature.[25]

2.2.1. Single-Component Permeation. For single-component permeation, the flux can be expressed by

$$J = -\epsilon\rho Đ\Gamma q^{sat}\frac{\partial\theta}{\partial z} = -\epsilon\rho Đ\Gamma\frac{\partial q}{\partial z} \quad \text{with } \Gamma = \frac{\partial \ln p}{\partial \ln q} \tag{4}$$

where $Đ$ is the Maxwell−Stefan diffusivity and Γ is the thermodynamic correction factor, which can be derived from an adsorption isotherm.

At steady state, the flux can be obtained by integrating eq 4 along the membrane coordinate z in combination with the Langmuir isotherm eq 1,

$$J = \frac{\epsilon\rho q^{sat}Đ}{\delta}\ln\left(\frac{1+Kp_r}{1+Kp_p}\right) \tag{5}$$

where δ is the thickness of the silicalite-1 layer and p_r and p_p are the partial pressures of the permeating species in the retentate and permeate streams, respectively.

At low pressures (corresponding to low loadings in the zeolite layer), eq 5 can be reformulated as follows,

$$J = \epsilon\rho K_H Đ\frac{\Delta p}{\delta} \quad \text{or} \quad \Pi = \frac{J}{\Delta p} = \frac{\epsilon\rho K_H Đ}{\delta} \tag{6}$$

where Δp is the difference in component pressure between the retentate and permeate streams and Π is the permeance. If the ideal selectivity (S_{ideal}) is defined as the ratio of single-component permeances at identical feed composition, at low pressures it can be expressed by

$$S_{ideal} = \frac{\Pi_1}{\Pi_2} = \frac{Đ_1 K_{H1}}{Đ_2 K_{H2}} \tag{7}$$

2.2.2. Binary-Mixture Permeation. The individual fluxes of components 1 and 2 in a binary system can be expressed by[25]

$$J_1 = -\epsilon\rho Đ_1 \frac{\left[\Gamma_{11}+\theta_1\frac{Đ_2}{Đ_{12}}(\Gamma_{11}+\Gamma_{21})\right]\frac{\partial q_1}{\partial z}+\left[\Gamma_{12}+\theta_1\frac{Đ_2}{Đ_{12}}(\Gamma_{12}+\Gamma_{22})\right]\frac{q_1^{sat}}{q_2^{sat}}\frac{\partial q_2}{\partial z}}{\theta_2\frac{Đ_1}{Đ_{12}}+\theta_1\frac{Đ_2}{Đ_{12}}+1} \tag{8}$$

with a similar relation for component 2. In eq 8, the exchange coefficient (diffusivity) $Đ_{12}$ is taken as the logarithmic average

of the Maxwell−Stefan diffusivities of the two components,

$$Đ_{12} = Đ_1^{\theta_1/(\theta_1+\theta_2)} Đ_2^{\theta_2/(\theta_1+\theta_2)} \quad (9)$$

as proposed originally by Krishna.[26] The values of the Γ_{ij} can be calculated from the binary isotherms for mixtures,

$$\Gamma_{ij} = \left(\frac{q_j^{sat}}{q_i^{sat}}\right)\frac{q_i}{p_i}\frac{\partial p_i}{\partial q_j}, \quad i,j = 1, 2 \quad (10)$$

Equation 8 is the so-called "full" GMS model. If the interaction between components 1 and 2 is not considered, the terms with $Đ_{12}$ vanish, leading to the following simplified equations,

$$J_1 = -\epsilon\rho Đ_1\left[\Gamma_{11}\frac{\partial q_1}{\partial z} + \Gamma_{12}\left(\frac{q_1^{sat}}{q_2^{sat}}\right)\frac{\partial q_2}{\partial z}\right] \quad (11)$$

with a similar relation for component 2.

The numerical calculation of the fluxes was done according to the method applied by Van de Graaf et al.[23]

3. Experimental Section

3.1. Adsorption Measurements. A Rupprecht and Patashnick tapered element oscillating microbalance (TEOM) 1500 mass analyzer (100 mg sample volume) was used to measure the isotherms of CH_4 and CO_2 on silicalite-1 crystals. A detailed description of the TEOM operating principles and isotherm measurements is given elsewhere.[27]

Prior to the experiments, the silicalite-1 crystals were outgassed in the following way. After a temperature rise with a rate of 10 K min^{-1} in situ in a He flow of 200 cm^3 (NTP) min^{-1} (normal temperature and pressure (NTP) = 298 K and 101.3 kPa), the sample was heated at 498 K for 2 h. The adsorption measurements were subsequently done at 303, 338, 373, and 408 K.

3.2. Silicalite-1 Membrane Synthesis. The silicalite-1 membrane was prepared by a two-step temperature synthesis during the crystallization. In the first step, the crystallization was performed at a lower temperature of 393 K for 114 h. Under these conditions, the nucleation was enhanced; consequently, small silicalite-1 crystals with dense population covered the support. The second-step synthesis was carried out at a higher temperature of 453 K for 17 h, which is favorable for fast crystal growth, filling the gaps between crystals in the membrane layer grown during the first-step synthesis. The molar ratio of the synthesis mixture was 100 SiO_2/59.3 TPABr/63.7 TPAOH/14 200 H_2O. TEOS was used as a silica source. The silicalite-1 membrane was grown from these reaction mixtures on a TRUMEM support (porous sintered stainless-steel disk with a diameter of 2.5 cm, a thickness of 250 μm, a mean pore size of 5 μm, and a porosity of 0.35). The as-synthesized silicalite-1 membrane was calcined in the following way: after a temperature rise at a rate of 0.5 K min^{-1} from room temperature, the sample was heated at 673 K in stagnant air for 16 h in order to remove the template inside the silicalite-1 crystals; then the sample was cooled to room temperature with a rate of 0.5 K min^{-1}. The membrane synthesis is remarkably reproducible, and the visual thickness of the silicalite-1 was ~20 μm, as determined from scanning electron microscopy (SEM).

3.3. Permeation Measurements. Permeation experiments were performed according to the Wicke−Kallenbach (WK) method. At the permeation side, He was used as a sweep gas with a flow rate of 100 cm^3 (NTP) min^{-1}. Before each measurement, He with a rate of 100 cm^3 (NTP) min^{-1} flowed at the feed and permeate sides of the membrane, and the module was heated at 408 K overnight to remove any adsorbed impurity. During the experiments reported here, either a pure feed gas or a mixture of the feed gas and He was used with a total flow rate of 100 cm^3 (NTP) min^{-1}. The silicalite-1 layer was facing the feed side. Feed, retentate, and permeate streams were analyzed with a mass spectrometer (Ledamass quadrupole analyzer). The detailed description of the setup and experimental procedures can be found elsewhere.[23]

Table 1. Summary of the Physical and Molecular Properties of the Components Investigated[a]

component	MW ($gmol^{-1}$)	LMV[b] (cm^3mol^{-1})	T_b (K)	σ_k[c] (nm)	α ($Å^3$)	μ (D)
CH_4	16.04	37.7	109.15	0.38	2.59	0
CO_2	44.01	33.3	194.65s[d]	0.33	2.91	0

[a] All data from ref 28 unless otherwise specified. [b] Liquid molar volume at normal boiling point. [c] Data from ref 29. [d] The "s" following this value indicates a sublimation point.

The ideal selectivity for CO_2 over CH_4 was defined as the ratio of the single-component permeances at the applied conditions, while the mixture selectivity for CO_2 was calculated as the quotient between two ratios of the molar fractions of CO_2 and CH_4 in the permeate and retentate streams.

The gaseous CO_2 and CH_4 were 3.5 grade (>99.95%). The physical and molecular properties of the components investigated are listed in Table 1.

4. Results and Discussion

4.1. Adsorption Isotherms. The isotherms of the pure components CH_4 and CO_2 on silicalite-1 crystals in the temperature range from 303 to 408 K and at pressures up to 500 kPa are shown in Figure 1. Some investigators[30−33] have used different techniques to determine the adsorption properties of CH_4 and CO_2 on silicalite-1. Sun et al.[30] used the gravimetric technique to measure the isotherms at temperatures ranging from 276 to 354 K and at pressures up to 2000 kPa. The measured highest loadings of CH_4 and CO_2 on silicalite-1 were 2.66 and 3.30 mol kg^{-1}, respectively, at 276 K. The isotherm data were correlated by a virial equation. Golden and Sircar[31] reported the isotherm data at 305 and 342 K and at pressures up to 1800 kPa, determined by a volumetric technique. These authors used the homogeneous multisite Langmuir model to describe the isotherm data. Rees et al.[32] also used a volumetric technique to investigate the adsorption properties of CH_4 and CO_2 on silicalite-1 in the temperature range from 273 to 323 K and at pressures up to 2000 kPa, and the isotherm data were correlated by the Langmuir model. Dunne et al.[33] reported the isotherm data at temperatures ranging from 313 to 334 K and at pressures up to 125 kPa, measured by a Tian−Calvet-type calorimeter. These authors did not correlate the data with any isotherm model.

In general, isotherm data at an individual temperature are described by one isotherm model; this is called the individual fitting. In this manner, the extracted saturation capacity will often vary with temperature.[34,35] For example, the saturation capacities from the individual Langmuir fitting for CH_4 and CO_2 on silicalite-1 decrease with temperature,[32] because of the increasing extrapolation with temperature. This behavior emphasizes a difficulty in applying the Langmuir model in a strict way, because available adsorption sites or volume should be constant and independent of operating temperature. With the

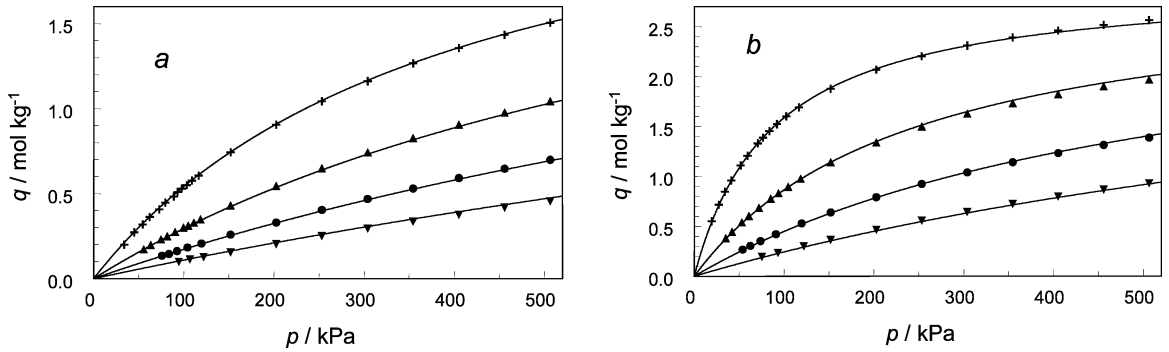

Figure 1. Adsorption isotherms of CH_4 and CO_2 on silicalite-1 crystals measured by the TEOM. The lines are the Langmuir model correlation: (a) CH_4; (b) CO_2; (+) 303 K; (▲) 338 K; (●) 373 K; (▼) 408 K.

Table 2. Estimated Parameter Values for the Combined Fitting of the Adsorption Data for Silicalite-1 by the Langmuir Model and Comparison with the Literature

component	q^{sat} (mol kg^{-1})	K_0 (kPa^{-1})	$-\Delta H_{ads}$ (kJ mol^{-1})	ref
CH_4	2.69 ± 0.01[a]	$(2.45 \pm 0.07) \times 10^{-6}$	17.5 ± 0.1	this study
	2.78 ± 0.02	$(5.80 \pm 0.84) \times 10^{-7}$	21.3 ± 0.4	30[b]
	2.44 ± 0.09	$(3.18 \pm 1.43) \times 10^{-7}$	23.3 ± 1.2	31[b]
	5.36		18.6	31[c]
	2.47−1.96	4.09×10^{-6}	16.5 (20.0)[d]	32[e]
	1.90 ± 0.03	$(5.04 \pm 0.33) \times 10^{-7}$	22.8 ± 0.2 (20.9)	33[b]
	4.5	2.21×10^{-7}	22.6	17[e]
CO_2	2.97 ± 0.01	$(5.62 \pm 0.17) \times 10^{-7}$	25.0 ± 0.1	this study
	3.21 ± 0.02	$(3.18 \pm 0.57) \times 10^{-7}$	26.0 ± 0.5	30[b]
	3.13 ± 0.03	$(5.05 \pm 1.75) \times 10^{-7}$	24.9 ± 0.9	31[b]
	5.00		24.1	31[c]
	3.84−2.95	2.85×10^{-6}	20.1 (24.6)	32[e]
	2.40 ± 0.05	$(2.54 \pm 0.52) \times 10^{-7}$	27.8 ± 0.6 (27.2)	33[b]
	2.48−1.46	2.74×10^{-7}	27.4	17[e]

[a] 95% confidence limit. [b] Parameter values extracted by the combined Langmuir isotherm fitting based on the isotherm data in the reference. [c] Parameter values for the multisite Langmuir model presented in the reference. [d] The value in parentheses represents the isosteric heat at zero coverage reported in the reference. [e] Parameter values derived by the individual Langmuir model fitting reported in the reference.

combined Langmuir fitting, the saturation capacity is one parameter for all temperatures and the temperature dependence of loading or coverage is expressed via the adsorption affinity parameter K.

The isotherm data can be well-described by the combined Langmuir fitting, as shown in Figure 1 by the drawn curves. The estimated parameter values are listed in Table 2. The extracted saturation capacity for CO_2 is higher than that for CH_4. This nearly quantitatively reflects the fact that the molar volume of CO_2 is smaller than that for CH_4 (Table 1). The K value at the same temperature is larger for CO_2 than CH_4. It implies that silicalite-1 has a higher adsorption affinity to CO_2. This is ascribed to the fact that the interaction between the adsorptive and the adsorbent is proportional to the polarizability, which is larger for CO_2 (Table 1).

Also, the reported isotherm data in the literature[30−33] can be described by the combined Langmuir fitting. The estimated parameters are presented in Table 2. Although the individual parameter values are slightly different, the calculated values of the Henry law constant K_H, which contains all three fitted parameters, are in good agreement, as shown in Figure 2. This indicates that the isotherm data in this study are accurate and reliable. Because of its simplicity in form and its correct behavior at low and high pressures, the Langmuir model is usually recommended as the first choice of isotherm equations for describing adsorption data. These Langmuir isotherms are used for modeling the permeation through the silicalite-1 membrane.

4.2. Single-Component Permeation. Figure 3 shows the single-component flux and permeance of either CH_4 or CO_2 as a function of feed pressure at 303 K. The temperature

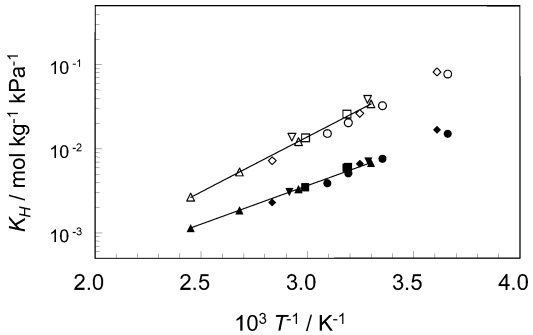

Figure 2. ln K_H vs $1/T$ plots for CH_4 and CO_2 on silicalite-1 crystals. Closed symbols are used for CH_4, and open symbols are used for CO_2: (▲, △) this study; (●, ○) data from Rees et al.;[32] (▼, ▽) data from Golden and Sircar;[31] (◆, ◇) data from Sun et al.;[30] (■, □) data from Dunne et al.[33]

dependence of the single-component flux and permeance at 101.3 kPa is presented in Figure 4. Both component fluxes increase with increasing feed pressures at 303 K, while the pressure dependence of their permeances shows an opposite trend. The flux and permeance of both components monotonically decrease with temperature over the investigated range (303−408 K). Bakker et al.[12] measured the permeances of CH_4 and CO_2 at 101 kPa between 200 and 650 K across silicalite-1 membranes using the WK method with He as a sweep gas. Their results were similar to those of Burggraaf et al.,[13] where the CO_2 flux exhibited a maximum near room temperature and a minimum at about 650 K and the CH_4 flux exhibited a maximum around 250 K and a minimum at 475 K. The current results at the applied conditions are in good agreement with those from Bakker et al.[12] and Burggraaf et al.[13] Kapteijn et al.[36] derived a diagnostic tool for unary-component permeation through

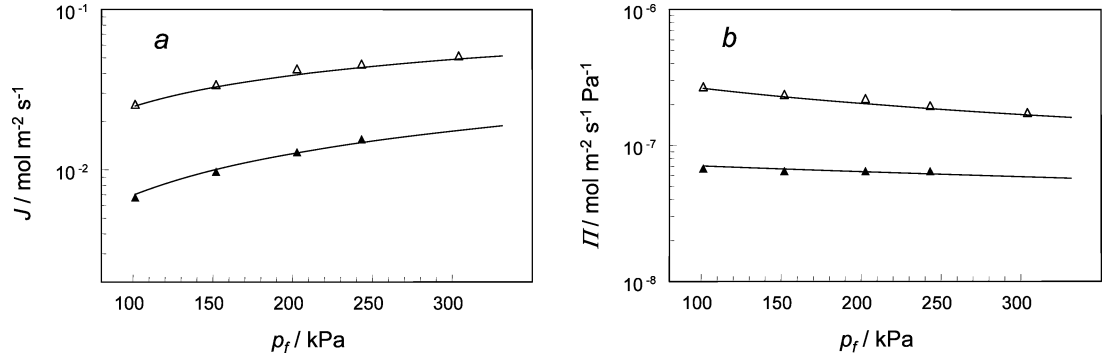

Figure 3. Unary flux and permeance of CH_4 and CO_2 as a function of feed pressure at 303 K through the silicalite-1 membrane (sweep gas He at the permeate side): (a) flux and (b) permeance. Closed symbols are used for CH_4, and open symbols are used for CO_2. The lines are the model simulations by eq 5.

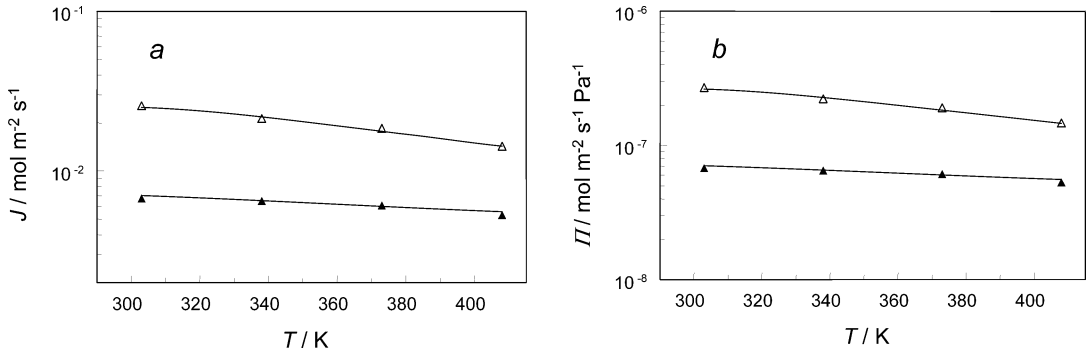

Figure 4. Unary flux and permeance of CH_4 and CO_2 as a function of temperature at a feed pressure of 101.3 kPa through the silicalite-1 membrane (sweep gas He at the permeate side): (a) flux and (b) permeance. Closed symbols are used for CH_4, and open symbols are used for CO_2. The lines are the model simulations by eq 5.

silicalite-1 membranes as a function of temperature, i.e., at a given pressure, the flux as a function of temperature is determined in terms of the difference between the apparent activated energy of diffusion and the heat of adsorption. The operating temperature not only affects the diffusivity but also the adsorption equilibrium constant. By increasing the operating temperature, the diffusivity becomes larger, inherently enhancing the permeation flux. On the other hand, the adsorption equilibrium constant becomes smaller, which leads to a lower occupancy in the zeolite. A decrease of loading in the zeolite will reduce the permeation flux. At lower temperatures, at which the adsorbed amount in the zeolite is higher, the enhancement of the diffusivity by increasing the temperature is dominant. In this temperature range, an increase in temperature accelerates the flux through the membrane. At a certain temperature, both effects, i.e., enhancement of the diffusivity and reduction of the loading by increasing temperature, become equal. At this temperature, a maximum in the plot of flux versus temperature appears, which is ascribed to these opposite temperature-dependent effects. By further increasing the temperature, the flux starts to decrease. In the investigated temperature range from 303 to 408 K, the effect of a decrease in loading with temperature on the permeation flux is dominant, which leads to a negative apparent permeation activation energy for both components, i.e., the flux decreases with temperature.

The ideal selectivity for CO_2 decreases with an increase in feed pressure at 303 K as well as with an increase in temperature at 101.3 kPa. These results are summarized in Figure 5.

It is difficult to make a comparison of the single-component fluxes in this study with the literature data. This difficulty is due to the fact that there is a significant difference in the thickness of the zeolite layer among synthesized membranes. On the other hand, the ideal selectivity should be less influenced by these factors, but the reported values of the ideal selectivity

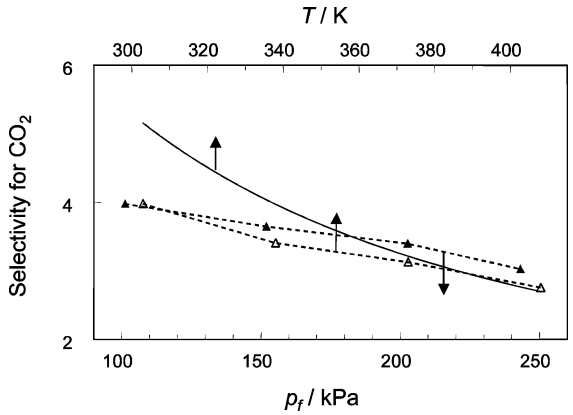

Figure 5. Ideal selectivity for CO_2 in the permeation through the silicalite-1 membrane. The closed symbols represent the selectivity as a function of feed pressure at 303 K, and the open symbols show the selectivity as a function of temperature at a feed pressure of 101.3 kPa. The dashed lines are to guide the eye, and the solid line represents the prediction by eq 7.

for the CO_2/CH_4 system vary over a wide range. At 101 kPa and ~300 K, Lovallo et al.[14] reported that the ideal selectivity for CO_2 over CH_4 was ~10 and Bakker et al.[12] and Van den Broeke et al.[17] reported a value of 1.2. The ideal selectivity was <1 at 300 K and at a feed pressure of 270 kPa and a constant pressure drop of 138 kPa across the membrane, reported by Poshusta et al.[15] In the current study, the ideal selectivity for CO_2 is ~4 at 303 K and 101.3 kPa. The selectivity for CH_4 found by Poshusta et al.[15] was due to the permeation partially through nonzeolites pores where viscous and Knudsen flow is dominant. Therefore, the ideal selectivity through a defect-free silicalite-1 membrane should be favorable for CO_2.

Knowing the values of the parameters ($\epsilon = 0.35$, $\delta = 2 \times 10^{-5}$ m, and $\rho = 1760$ kg m^{-3}), the component partial pressures at the retentate and permeate sides, and the adsorption param-

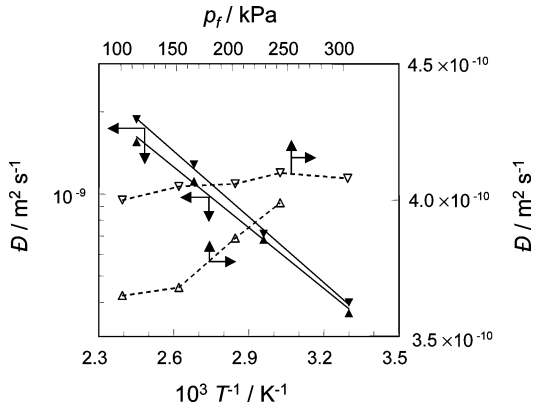

Figure 6. Diffusivities of CH_4 and CO_2 estimated from the permeation through the silicalite-1 membrane. Closed symbols show the data as a function of temperature at a feed pressure of 101.3 kPa; open symbols show the data as a function of feed pressure at 303 K. The lines are the fits by the Arrhenius equation, and the dashed lines are to guide the eye: (▲, △) CH_4; (▼, ▽) CO_2.

Table 3. Diffusion Parameters in the Arrhenius Plot for CH_4 and CO_2 in the Silicalite-1 Membrane Layer and Literature Values Determined from the WK Membrane Permeation

	CH_4		CO_2		
p_f (kPa)	$Đ_0$ (10^{-7} m^2 s^{-1})	E_a (kJ mol^{-1})	$Đ_0$ (10^{-7} m^2 s^{-1})	E_a (kJ mol^{-1})	ref
101.3	1.07	14.2	1.76	15.4	this study
101.3	0.39	8.8	0.07	9.6	12
1.15−1.22	2.32	10.8			44[a]
101.3	0.136	6.6			45

[a] Determined from the permeation flux through a single-crystal membrane.

eters (Table 2), the diffusivities were calculated using eq 5 and are summarized in Figure 6. At 303 K, the Maxwell−Stefan diffusivities for CO_2 are practically constant at different feed pressures, while those for CH_4 slightly increase with feed pressure. This experimental finding may be understood with the concepts "surface resistance" and "evaporation barrier" on encountering the crystal surface from the intracrystalline space originally proposed by Barrer[37] and Kärger.[38] These transport resistances can be caused by a relaxation of the crystal structure in the surface layer or at crystal intergrowths. Recently, a molecular simulation study confirms the presence of these surface resistances.[39−42] Simulation results indicated that the effect of molecular size is more important to determine the magnitude of surface resistances compared to the energy effect, as a small difference in size causes large differences in the magnitude of resistances.[41] Furthermore, the range of the surface resistance is primarily a function of molecular size: for smaller molecules, the range of the surface resistance becomes shorter than that for larger molecules. In addition, the magnitude of the surface resistance decreases as the pressure increases. Zhu et al.[43] pointed out that the pressure-dependent Đ for 3-methylpentane through this silicalite-1 membrane could be attributed to intercrystalline barriers in the membrane. Because of their larger molecular size compared to CO_2, CH_4 molecules more strongly experience the intercrystalline barriers, and with increasing pressure, the influence of these barriers decreases, leading to an apparent increase in Đ with feed pressure.

The temperature dependence of the diffusivity estimated from the unary permeation at a feed pressure of 101.3 kPa seems to follow the Arrhenius law; see Figure 6. The derived diffusivity parameters are included in Table 3. It is clear to see that both components have similar transport properties through the membrane. For comparison, the literature data determined from WK membrane permeations are also presented in Table 3. In the current study, both diffusional activation energy E_a and preexponential coefficient $Đ_0$ deviate from the literature results.[12,44] The difference between the current result for CH_4 and the data from Talu et al.[44] may be related to different membrane morphologies. A layer of intergrown crystals was used in the current study, while Talu et al.[44] used a single crystal for determining the diffusivities. Additionally, the technique used by Talu et al. was to measure a directional diffusivity in the *z*-direction, which usually leads to a higher value of the determined diffusivity. A higher value of E_a for CH_4 in this study, compared to the literature,[44,45] indicates the presence of the intercrystalline barriers in the current membrane.

Kapteijn et al.[46] made a comparison of CH_4 diffusivities at ~300 K determined by different techniques. The reported diffusivities are in the range from 1.3×10^{-14} m^2 s^{-1} determined by chromatography to 1.4×10^{-8} m^2 s^{-1} determined by molecular simulation. The CH_4 diffusivities determined by the membrane technique are in the range from 1.1×10^{-10} to 3.2×10^{-9} m^2 s^{-1}. The current result (3.65×10^{-10} m^2 s^{-1}) is on the low side but is in reasonable agreement with 5.0×10^{-10} m^2 s^{-1} from Gardner et al.[20], determined by transient measurements in H-ZSM-5 membranes. However, note that absolute diffusivity values are strongly determined by the choice of the ill-defined membrane thickness. Compared with CH_4, much less data are available for CO_2. Gardner et al.[20] found that the diffusivity of CO_2 at 298 K and a feed pressure of 117 kPa was 1.7×10^{-10} m^2 s^{-1}, which is lower than 4.0×10^{-10} m^2 s^{-1} at 303 K and a feed pressure of 101.3 kPa in this study. In contrast to the current observation, under similar conditions, the diffusivities from Gardner et al.[20] are higher for CH_4 than for CO_2. This discrepancy is probably due to the different types of membrane used (silicalite-1 and H-ZSM-5). Additionally, in the transient measurements by Gardner et al., the adsorption parameters and Maxwell−Stefan diffusivity were simultaneously estimated, and any changes in the adsorption parameters would pass on the determined diffusivity. Similar to the current trend, Gardner et al.[20] also observed that the derived diffusivities for CH_4 had a more-pronounced pressure dependence.

By employing the obtained adsorption and diffusion parameters presented in Tables 2 and 3, the fluxes and permeances are simulated and shown in Figures 3 and 4 by the solid lines. These simulation results are in good agreement with experimental data. In Figure 5, the line represents the theoretical curve calculated from eq 7 for the ideal selectivity in the linear adsorption range as a function of temperature. The good agreement between theoretical prediction and experimental observation at high temperatures, at which the adsorption is in the Henry law range, confirms the validation of eq 7 for predicting the limiting (maximum) ideal selectivity.

4.3. Binary Permeation. Figure 7 represents the component fluxes of a CO_2 and CH_4 (50:50) mixture as a function of total feed pressure and of temperature. Both component fluxes increase with total feed pressure at 303 K. At 101.3 kPa in the binary permeation, the CO_2 flux monotonically decreases with temperature over the investigated range, while the CH_4 flux first increases with temperature up to 338 K and then slightly decreases with temperature. The mixture selectivity is almost constant with an increase in total feed pressure at 303 K, although there is a trend to slightly decrease, while it significantly decreases with temperature at a total feed pressure of 101.3 kPa. The latter is in qualitative agreement with the observation from Lovallo et al.,[14] Poshusta et al.,[15] and Van den Broeke et al.[18] These results are shown in Figure 8. The

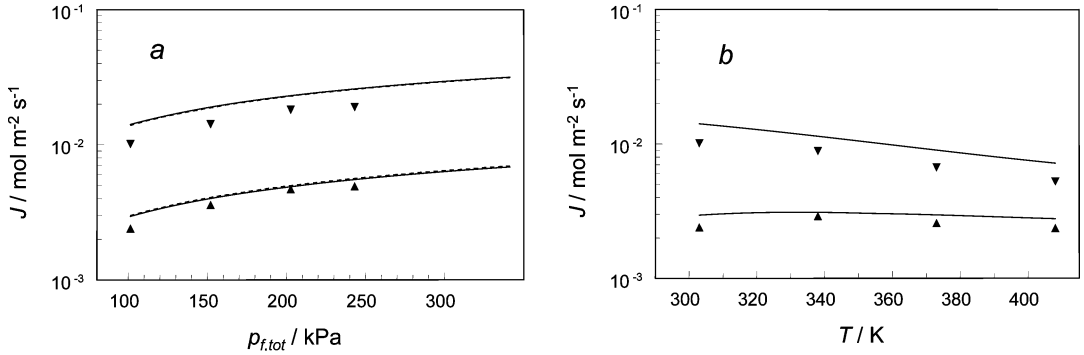

Figure 7. Component fluxes of the binary (50:50) mixture of CH_4 and CO_2 through the silicalite-1 membrane: (a) as a function of the total feed pressure at 303 K; (b) as a function of temperature at a total feed pressure of 101.3 kPa. The solid lines are the full model predictions by eq 8, and the dashed lines are the simplified predictions by eq 11.

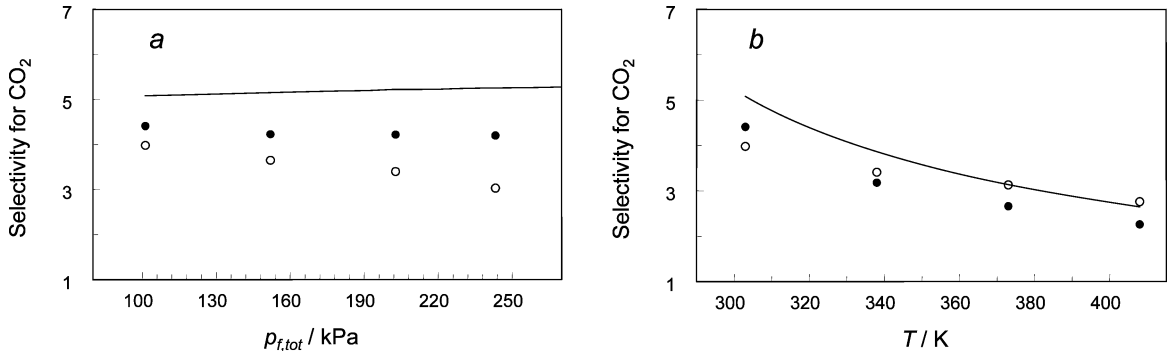

Figure 8. Mixture permeation selectivity for CO_2 based on the data of Figure 7: (a) as a function of the total feed pressure at 303 K; (b) as a function of temperature at a total feed pressure of 101.3 kPa; open symbols indicate the ideal selectivity. The lines are the model predictions by eq 8.

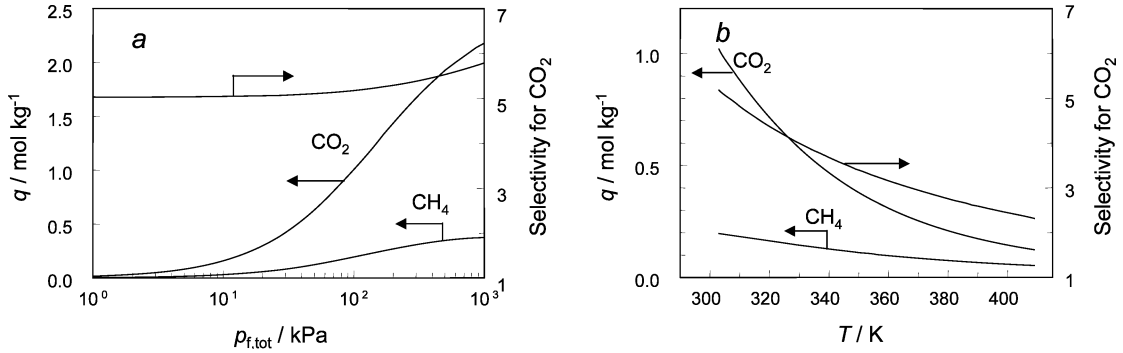

Figure 9. Binary (50:50) IAS isotherms and mixture adsorption selectivity for CO_2: (a) as a function of the total feed pressure at 303 K; (b) as a function of temperature at a total feed pressure of 101.3 kPa.

mixture selectivity as a function of total feed pressure at 303 K is higher than the ideal selectivity, but the temperature-dependent mixture selectivity at a total feed pressure of 101.3 kPa is almost identical to the ideal selectivity. Lovallo et al.[14] found that the ideal and mixture selectivities as a function of temperature were similar, which is in good agreement with the current observation. Posthusta et al.,[15] however, observed that the ideal selectivity was favorable for CH_4 while the mixture selectivity for CO_2 over CH_4 was as high as 5.5 at 303 K. This apparently deviates from the current observation. Basically, if the permeation through nonzeolite pores results in ideal selectivity for CH_4, the mixture selectivity should also be favorable for CH_4.

Using the adsorption parameters in Table 2 and the diffusivities determined from the unary permeation at a feed pressure of 101.3 kPa in Table 3, the GMS equations in combination with the IAST were used to predict the binary permeation. The predictions by the full model and the simplified one, i.e., eq 11, are identical, as shown in Figure 7a. This is the case for facile molecule−molecule exchange, i.e., numerically $Đ_{12} \rightarrow \infty$, in which vacancy correlation effects tend to get washed out.[47]

Figures 7 and 8 show a comparison of the experimental data with the model predictions. The model predictions are in good agreement with the experimental data for CH_4. Experimentally, the CH_4 flux slightly increases with temperature up to 338 K at 101.3 kPa, and the model predicts the same trend, shown in Figure 7b. On the other hand, the model slightly overpredicts the flux of CO_2 in the whole temperature or pressure range investigated. Consequently, higher mixture selectivities are predicted by the model, compared to those from the measurements, as shown in Figure 8. In addition, the predicted mixture selectivity at 303 K slightly increases with total feed pressure, while the experimental observation shows an opposite trend. There are two plausible reasons for the deviation. One may be related to the mixture adsorption predicted by the IAST. Figure 9 shows the IAST predictions for the binary isotherms and selectivities of a CH_4 and CO_2 (50:50) mixture on silicalite-1 as a function of temperature and pressure. The mixture adsorption selectivity decreases with temperature at a total feed pressure of 101. kPa, which is consistent with both experimental observation and model prediction in the binary permeation. At

303 K, the binary adsorption selectivity for CO_2 is quite constant at lower total feed pressures, while it increases with pressure in a higher-pressure range. In the IAST, an ideal solution in the adsorbed phase and a perfect gas phase are assumed. At high pressures, corresponding to high loadings on the adsorbent, both assumptions may be doubtful. The overprediction of the CO_2 flux and the binary permeation selectivity could be caused by the overestimation of the CO_2 loading in the zeolite by the IAST. If more accurate binary adsorption models are available, some improvements in prediction will be possible.

The second reason for the deviation may be related to the pressure-dependent diffusivity for CH_4. As discussed before, the diffusivity of the smaller molecule CO_2 is independent of feed pressure, while it apparently increases with pressure for CH_4, due to some intercrystalline barriers. This may lead to a decrease in the binary permeation selectivity experimentally. These effects result in the deviation of the model prediction from the experimental observation.

Van den Broeke et al.[18] experimentally observed that the binary permeation selectivity for CO_2 at 303 K decreased from 2.5 at 100 kPa to 1.5 at 900 kPa, which is lower compared to the current results under the same conditions. These lower selectivities could be caused by support effects. The support of the WTSS-1 membrane was much thicker (3 mm thick porous sintered stainless-steel support coated with a 50−150 μm smooth top layer of metal wool)[17,18] than the TRUMEN support used in the current study. For a zeolite membrane coated on such a thick support, the mass-transfer resistance through the support has to be taken into account,[23] which was not done by Van den Broeke and co-workers.[17,18] The support selectivity is more favorable for methane, counteracting that of the zeolite layer and resulting in an opposite trend, a phenomenon observed by Van de Graaf et al.[23] for methane/ethane mixtures. Van den Broeke et al.[18] also used the GMS equations with the IAST to predict the mixture selectivity. Exceptionally, their model prediction shows a similar trend as the experimental observation. This could be caused by the pure-component adsorption data that was used. As shown in Table 2, at 303 K in their study ,the isotherm of CH_4 on silicalite-1 was measured with an isobaric technique below 1 bar, and the extracted value of the saturation capacity was 4.5 mol kg^{-1}, which is much higher than the theoretical value from a molecular simulation[35] due to the large extrapolation. Van den Broeke et al.[17] also used the TEOM technique to measure the isotherm data of CO_2, but the silicalite-1 sample used was different from that in the current study. The silicalite-1 had been calcined at 723 K, at which temperature template fragments were not completely removed,[34] resulting in a lower adsorption capacity (by ~20%) for CO_2, compared to the current value. These could affect the model prediction and lead to a different trend in the binary permeation selectivity. In addition, the authors assumed that the component concentrations at the permeate side were zero in their simulation,[18] which was an oversimplification.

The approach followed here to model the mixture permeation is based on the adsorption data and the unary permeation determined separately. The adsorption in the silicalite-1 layer plays an important role in the separation performance. The accuracy of adsorption data is crucial in the permeation modeling. Although there are some small differences between model prediction and experimental observation, the GMS equations in combination with the IAST enable one to predict the binary permeation.

In general, intercrystalline barriers in zeolite membranes should be eliminated, because they can reduce component fluxes. However, the current study indicates that these barriers can lead to some benefits for CO_2/CH_4 separation. The larger CH_4 molecules are affected by the intercrystalline barriers while the smaller CO_2 molecules are not, resulting in a higher selectivity for CO_2. In the case of molecular sieving, e.g., with intracrystalline barriers, the smaller the aperture size of the pore in the membrane, the higher is the selectivity for CO_2. Recently, Tomita et al.[9] reported that the separation factors for CO_2 in a CO_2 and CH_4 (50:50) mixture through a DD3R membrane were as high as 220 and 100 at 301 and 373 K, respectively, at a total feed pressure of 500 kPa. Although the eight-ring windows of DD3R zeolite are accessible to both CO_2 and CH_4 molecules, the favored adsorption and transport for CO_2 in the DD3R zeolite layer lead to the high separation performance.

5. Conclusions

Accurate adsorption isotherm data of CH_4 and CO_2 on silicalite-1 crystals were measured with the TEOM at temperatures ranging from 303 to 408 K and at pressures up to 500 kPa. This was confirmed by an extensive comparison with reliable literature data determined by other techniques. All isotherm data, including those in the literature, can be well-described by the combined Langmuir model fitting. The single and binary permeation of CH_4 and CO_2 through a silicalite-1 membrane was measured as a function of temperature and feed pressure. Both ideal and mixture permeation selectivities are favorable for CO_2 because of a higher adsorption affinity of the zeolite to CO_2. The diffusivity of CH_4 estimated from its single-component permeation shows a weak pressure dependence, which could be ascribed to the intercrystalline barriers in the intergrown silicalite-1 crystal layer. These barriers, in turn, lead to a better performance for CO_2/CH_4 separation but decrease the CO_2 selectivity with increasing pressure. The GMS equations in combination with the IAST enable one to predict the binary permeation. The use of accurate adsorption data is of utmost importance for extracting transport properties from the single-component permeation as well as for modeling multicomponent permeation.

Nomenclature

$Đ$ = diffusivity (m^2 s^{-1})
$Đ_0$ = diffusivity at infinite temperature (m^2 s^{-1})
$Đ_{12}$ = exchange diffusivity defined by eq 9 (m^2 s^{-1})
E_a = diffusivity activation energy (kJ mol^{-1})
K = adsorption equilibrium constant (kPa^{-1})
K_0 = adsorption equilibrium constant at infinite temperature (kPa^{-1})
K_H = Henry law constant (mol kg^{-1} kPa^{-1})
J = flux (mol m^{-2} s^{-1})
LMV = liquid molar volume at normal boiling point (cm^3 mol^{-1})
MW = Molecular weight (g mol^{-1})
p = pressure (kPa)
q = amount adsorbed (mol kg^{-1})
q^{sat} = saturation amount adsorbed (mol kg^{-1})
R_g = universal gas constant (8.314 J mol^{-1} K^{-1})
S_{ideal} = ideal selectivity
t = time (s)
T = temperature (K)
T_b = boiling point at 101.3 kPa (K)
z = space coordinate (m)

Greek Symbols

α = molecular polarizability (Å^3)
ϵ = porosity in the support layer
μ = molecular dipole moment (Debye)
δ = thickness of the zeolite layer (μm)
θ = fractional occupancy
ρ = zeolite density (kg m^{-3})
σ_k = kinetic diameter (nm)
Δp = difference in pressure between retentate and permeate sides (kPa)
ΔH_{ads} = adsorption enthalpy (kJ mol^{-1})
Γ = thermodynamic correction factor
Π = permeance (mol m^{-2} s^{-1} Pa^{-1})

Subscripts

1, 2 = components 1, 2
f = feed
f,tot = total feed
i, *j* = components *i*, *j*
p = permeate side
r = retentate side

Literature Cited

(1) Koros, W. J.; Mahajan, R. Pushing the limits on possibilities for large scale gas separation: Which strategies? *J. Membr. Sci.* **2001**, *175*, 181.

(2) Koros, W. J.; Fleming, G. K. Membrane-based gas separation. *J. Membr. Sci.* **1993**, *83*, 1.

(3) Poshusta, J. C.; Tuan, V. A.; Falconer, J. L.; Noble, R. D. Synthesis and permeation properties of SAPO-34 tubular membranes. *Ind. Eng. Chem. Res.* **1998**, *37*, 3924.

(4) Poshusta, J. C.; Tuan, V. A.; Pape, E. A.; Noble, R. D.; Falconer, J. L. Separation of light gas mixtures using SAPO-34 membranes. *AIChE J.* **2000**, *46*, 779.

(5) Poshusta, J. C.; Noble, R. D.; Falconer, J. L. Characterization of SAPO-34 membranes by water adsorption. *J. Membr. Sci.* **2001**, *186*, 25.

(6) Li, S. G.; Falconer, J. L.; Noble, R. D. SAPO-34 membranes for CO_2/CH_4 separation. *J. Membr. Sci.* **2004**, *241*, 121.

(7) Li, S. G.; Alvarado, G.; Noble, R. D.; Falconer, J. L. Effects of impurities on CO_2/CH_4 separations through SAPO-34 membranes. *J. Membr. Sci.* **2005**, *251*, 59.

(8) Li, S. G.; Martinek, J. G.; Falconer, J. L.; Noble, R. D.; Gardner, T. Q. High-pressure CO_2/CH_4 separation using SAPO-34 membranes. *Ind. Eng. Chem. Res.* **2005**, *44*, 3220.

(9) Tomita, T.; Nakayama, K.; Sakai, H. Gas separation characteristics of DDR type zeolite membrane. *Microporous Mesoporous Mater.* **2004**, *68*, 71.

(10) Yan, Y.; Davis, M. E.; Gavalas, G. R. Preparation of zeolite ZSM-5 membranes by in-situ crystallization on porous α-Al_2O_3. *Ind. Eng. Chem. Res.* **1995**, *34*, 1652.

(11) Kusakable, K.; Yoneshige, S.; Murata, A.; Morooka, S. Morphology and gas permeance of ZSM-5-type zeolite membrane formed on a porous α-alumina support tube. *J. Membr. Sci.* **1996**, *116*, 39.

(12) Bakker, W. J. W.; Van den Broeke, L. J. P.; Kapteijn, F.; Moulijn, J. A. Temperature dependence of one-component permeation through a silicalite-1 membrane. *AIChE J.* **1997**, *43*, 2203.

(13) Burggraaf, A. J.; Vroon, Z. A. E. P.; Keizer, K.; Verweij, H. Permeation of single gases in thin zeolite MFI membranes. *J. Membr. Sci.* **1998**, *144*, 77.

(14) Lovallo, M. C.; Gouzinis, A.; Tsapatsis, M. Synthesis and characterization of oriented MFI membranes prepared by secondary growth. *AIChE J.* **1998**, *44*, 1903.

(15) Poshusta, J. C.; Noble, R. D.; Falconer, J. L. Temperature and pressure effects on CO_2 and CH_4 permeation through MFI zeolite membranes. *J. Membr. Sci.* **1999**, *160*, 115.

(16) Hedlund, J.; Noack, M.; Kölsch, P.; Creaser, D.; Caro, J.; Sterte, J. ZSM-5 membranes synthesized without organic templates using a seeding technique. *J. Membr. Sci.* **1999**, *159*, 263.

(17) Van den Broeke, L. J. P.; Bakker, W. J. W.; Kapteijn, F.; Moulijn, J. A. Transport and separation properties of a silicalite-1 membrane. I. Operating conditions. *Chem. Eng. Sci.* **1999**, *54*, 245.

(18) Van den Broeke, L. J. P.; Kapteijn, F.; Moulijn, J. A. Transport and separation properties of a silicalite-1 membrane. II. Variable separation factor. *Chem. Eng. Sci.* **1999**, *54*, 259.

(19) Takata, Y.; Tsuru, T.; Yoshioka, T.; Asaeda, M. Gas permeation properties of MFI zeolite membranes prepared by the secondary growth of colloidal silicalite and application to the methylation of toluene. *Microporous Mesoporous Mater.* **2002**, *54*, 257.

(20) Gardner, T. Q.; Flores, A. I.; Noble, R. D.; Falconer, J. L. Transient measurements of adsorption and diffusion in H-ZSM-5 membranes. *AIChE J.* **2002**, *48*, 1155.

(21) Algieri, C.; Bernardo, P.; Golemme, G.; Barbieri, G.; Drioli, E. Permeation properties of a thin silicalite-1 (MFI) membrane. *J. Membr. Sci.* **2003**, *222*, 181.

(22) Bonhomme, F.; Welk, M. E.; Nenoff, T. M. CO_2 selectivity and lifetimes of high silica ZSM-5 membranes. *Microporous Mesoporous Mater.* **2003**, *66*, 181.

(23) Van de Graaf, J. M.; Kapteijn, F.; Moulijn, J. A. Modeling permeation of binary mixtures through zeolite membranes. *AIChE J.* **2000**, *46*, 497.

(24) Myers, A. L.; Prausnitz, J. M. Thermodynamics of mixed-gas adsorption. *AIChE J.* **1965**, *11*, 121.

(25) Kapteijn, F.; Moulijn, J. A.; Krishna, R. The generalized Maxwell−Stefan model for diffusion in zeolites: Sorbate molecules with different saturation loadings. *Chem. Eng. Sci.* **2000**, *55*, 2923.

(26) Krishna, R. Multicomponent surface-diffusion of adsorbed species—A description based on the generalized Maxwell−Stefan equations. *Chem. Eng. Sci.* **1990**, *45*, 1779.

(27) Zhu, W.; Van de Graaf, J. M.; Van den Broeke, L. J. P.; Kapteijn, F.; Moulijn, J. A. TEOM: A unique technique for measuring adsorption properties. Light alkanes in silicalite-1. *Ind. Eng. Chem. Res.* **1998**, *37*, 1934.

(28) Lide, D. R. *CRC Handbook of Chemistry and Physics*, 81st ed.; CRC Press: Boca Raton, FL, 2001.

(29) Breck, D. W. *Zeolite Molecular Sieves—Structure, Chemistry, and Use*; Wiley: New York, 1974.

(30) Sun, M. S.; Shah, D. B.; Xu, H. H.; Talu, O. Adsorption equilibria of C_1 to C_4 alkanes, CO_2, and SF_6 on silicalite. *J. Phys. Chem. B* **1998**, *102*, 1466.

(31) Golden, T. C.; Sircar, S. Gas adsorption on silicalite. *J. Colloid Interface Sci.* **1994**, *162*, 182.

(32) Rees, L. V. C.; Brückner, P.; Hampson, J. Sorption of N_2, CH_4, and CO_2 in silicalite-1. *Gas Sep. Purif.* **1991**, *5*, 67.

(33) Dunne, J. A.; Mariwala, R.; Rao, M.; Sircar, S.; Gorte, R. J.; Myers, A. L. Calorimetric heats of adsorption and adsorption isotherms. 1. O_2, N_2, Ar, CO_2, CH_4, C_2H_6, and SF_6 on silicalite. *Langmuir* **1996**, *12*, 5888.

(34) Zhu, W.; Kapteijn, F.; Moulijn, J. A. Equilibrium adsorption of light alkanes in silicalite-1 by the inertial microbalance technique. *Adsorption* **2000**, *6*, 159.

(35) Zhu, W.; Kapteijn, F.; Moulijn, J. A. Adsorption of light alkanes on silicalite-1: Reconciliation of experimental data and molecular simulations. *Phys. Chem. Chem. Phys.* **2000**, *2*, 1989.

(36) Kapteijn, F.; Van de Graaf, J. M.; Moulijn, J. A. One-Component permeation maximum: Diagnostic tool for silicalite-1 membranes? *AIChE J.* **2000**, *46*, 1096.

(37) Barrer, R. M. Flow into and through zeolite beds and compacts. *Langmuir* **1987**, *3*, 309.

(38) Kärger, J. Mass transfer through beds of zeolite crystallites and the paradox of the evaporation barrier. *Langmuir* **1988**, *4*, 1289.

(39) Arya, G.; Maginn, E. J.; Chang, H. C. Effect of the surface energy barrier on sorbate diffusion in $AlPO_4$-5. *J. Phys. Chem. B* **2001**, *105*, 2725.

(40) Arya, G.; Chang, H. C.; Maginn, E. J. A critical comparison of equilibrium, nonequilibrium and boundary-driven molecular dynamics techniques for studying transport in microporous materials. *J. Chem. Phys.* **2001**, *115*, 8112.

(41) Ahunbay, M. G.; Elliott, J. R.; Talu, O. Surface resistance to permeation through the silicalite crystal membrane: Variation with permeant. *J. Phys. Chem. B* **2004**, *108*, 7801.

(42) Newsome, D. A.; Sholl, D. S. Predictive assessment of surface resistances in zeolite membranes using atomically detailed models. *J. Phys. Chem. B* **2005**, *109*, 7237.

(43) Zhu, W.; Hrabanek, P.; Gora, L.; Kapteijn, F.; Jansen, J. C.; Moulijn, J. A. Modelling of *n*-hexane and 3-methylpentane permeation through a silicalite-1 membrane. *Stud. Surf. Sci. Catal.* **2004**, *154*, 1935.

(44) Talu, O.; Sun, M. S.; Shah, D. B. Diffusivities of *n*-alkanes in silicalite by steady-state single-crystal membrane technique. *AIChE J.* **1998**, *44*, 681.

(45) Van de Graaf, J. M.; Kapteijn, F.; Moulijn, J. A. Diffusivities of light alkanes in a silicalite-1 membrane layer. *Microporous Mesoporous Mater.* **2000**, *35*−*36*, 267.

(46) Kapteijn, F.; Bakker, W. J. W.; Zheng, G.; Poppe, J.; Moulijn, J. A. Permeation and separation of light hydrocarbons through a silicalite-1 membrane. Application of the generalized Maxwell−Stefan equations. *Chem. Eng. J.* **1995**, *57*, 145.

(47) Krishna, R.; Baur, R. Analytic solution of the Maxwell−Stefan equations for multicomponent permeation across a zeolite membrane. *Chem. Eng. J.* **2004**, *97*, 37.

Received for review June 21, 2005
Revised manuscript received October 7, 2005
Accepted October 18, 2005

IE0507427